



Adipose-Derived Neural Stem Cells Combined with Acellular Dermal Matrix as a Neural Conduit Enhances Peripheral Nerve Repair

Wei-Ze Syu¹, Dueng-Yuan Hueng^{2,3}, Wei-Liang Chen⁴, James Yi-Hsin Chan^{1,5}, Shyi-Gen Chen^{1,6}, and Shih-Ming Huang^{1,2} 

Cell Transplantation
2019, Vol. 28(9-10) 1220–1230
© The Author(s) 2019
Article reuse guidelines:
sagepub.com/journals-permissions
DOI: 10.1177/0963689719853512
journals.sagepub.com/home/cll


Abstract

Reconstruction to close a peripheral nerve gap continues to be a challenge for clinical medicine, and much effort is being made to develop nerve conduits facilitate nerve gap closure. Acellular dermal matrix (ADM) is mainly used to aid wound healing, but its malleability and plasticity potentially enable it to be used in the treatment of nerve gaps. Adipose-derived stem cells (ADSCs) can be differentiated into three germ layer cells, including neurospheres. We tested the ability of ADSC-derived neural stem cells (NSCs) in combination with ADM or acellular sciatic nerve (ASN) to repair a transected sciatic nerve. We found that NSCs form neurospheres that express Nestin and Sox2, and could be co-cultured with ADM *in vitro*, where they express the survival marker Ki67. Following sciatic nerve transection in rats, treatment with ADM+NSC or ASN+NSC led to increases in relative gastrocnemius weight, cross-sectional muscle fiber area, and sciatic functional index as compared with untreated rats or rats treated with ADM or ASN alone. These findings suggest that ADM combined with NSCs can improve peripheral nerve gap repair after nerve transection and may also be useful for treating other types of neurological gaps.

Keywords

acellular dermal matrix, adipose-derived stem cells, nerve engineering, peripheral nerve gap repair

Introduction

A nerve gap is defined as the distance between the ends of a completely severed nerve^{1,2}. If a nerve gap is relatively small, end-to-end repair is the preferred treatment, but sometimes the axons cannot cross the scar tissue in the wound area^{3,4}. Nonetheless, though it remains a major challenge, thanks to advances in precision microsurgery and greater understanding of neurophysiological and molecular pathways, peripheral nerve repair is no longer an unattainable fantasy.

Autologous nerve transplantation is currently the most effect approach to repair of wide nerve gaps, but autologous nerve grafts are limited by donor sensory loss, the length of the nerve defect site, the size of the defect nerve, and the fact that deficient nerve type may differ from that of the nerve graft. All of these factors can reduce the efficacy of the procedure^{5,6}. To overcome these shortcomings, the development of biosynthetic material nerve conduits has been actively pursued, and choices available for nerve gap repair are now more diverse. The current US FDA-approved nerve

¹ Graduate Institute of Life Sciences, National Defense Medical Center, Taipei

² Department of Biochemistry, National Defense Medical Center, Taipei

³ Department of Neurological Surgery, Tri-Service General Hospital, National Defense Medical Center, Taipei

⁴ Division of Family Medicine, Department of Family and Community Medicine, Tri-Service General Hospital, and School of Medicine, National Defense Medical Center, Taipei

⁵ Superintendent's Office, National Defense Medical Center, Taipei

⁶ Division of Plastic and Reconstructive Surgery, Tri-Service General Hospital, National Defense Medical Center, Taipei

*This article was originally submitted for PPSSC issue

Submitted: March 9, 2019. Revised: April 23, 2019. Accepted: May 2, 2019.

Corresponding Authors:

James Yi-Hsin Chan, Superintendent's Office, National Defense Medical Center, Taipei 114.

Email: jchan9473@gmail.com

Shyi-Gen Chen, Division of Plastic and Reconstructive Surgery, Tri-Service General Hospital, National Defense Medical Center, Taipei 114.

Email: shyigen@gmail.com

Shih-Ming Huang, Department of Biochemistry, National Defense Medical Center, 161, MinChuan East Road, Section 6, Taipei 114.

Email: shihming@ndmctsgh.edu.tw



conduit is composed of collagen and polyglycolic acid or polycaprolactone.

Advances in medical technology and proper treatment of acellular tissue that preserves its original structure could reduce the immune response to allogeneic transplantation. This gives acellular tissue great potential for application in clinical medicine⁵. An advantage of acellular nerves is that they provide extracellular matrix molecules such as fibronectin and laminin, which support and enhance nerve regeneration^{7,8}. For example, the extent of repair achieved using acellular sciatic nerve (ASN) was significantly greater than that achieved using a silicone nerve conduit⁹.

Schwann cells exhibit different phenotypes at different times during the nerve repair process, and release related neurotrophic factors to help nerve repair^{10,11}. The inability to obtain sufficient Schwann cells in a short period of time severely limits their clinical application¹⁰. Neural stem cells (NSCs) are stem cells capable of differentiating into neurons or glial cells. Studies have shown that NSC implantation is beneficial in cases of acute or chronic peripheral nerve injury¹². However, NSCs are associated with a higher rate of neuroblastoma formation and the primary source is the brain¹³. Adipose-derived stem cells (ADSCs) can be obtained through conventional procedures such as liposuction, and the number of ADSCs obtained per unit adipose tissue is much higher than with other types of stem cells. Moreover, ADSCs have greater proliferation and differentiation potential than mesenchymal stem cells¹⁴, and they can be induced into NSCs by adding equal portions of epidermal growth factor (EGF) and fibroblast growth factor (FGF) to a specific medium¹⁵.

Currently, acellular dermal matrix (ADM) is used primarily for research into healing severe wounds such as burns and chronic wounds¹⁶⁻¹⁸, and its *in vivo* metabolism and microstructure are well established¹⁹⁻²². The ductility and plasticity of ADM suggest that it is potentially useful for repair of nerve gaps of various sizes in nerves of different diameters, and that it could be combined with neuro-engineered materials for future benefits to patient. We previously showed that ADSCs can be induced into NSCs, which can grow on ADM²³. In the present study, we present several lines of evidence that ADM combined with ADSC-derived NSCs can contribute to nerve gap repair in a rat model of sciatic nerve transection with a 10-mm gap. These findings provide new insight into a nerve repair strategy for patients with a peripheral nerve injury.

Materials and Methods

Isolation and Culture of ADSCs

ADSCs were collected from healthy donors at the Tri-Service General Hospital, Taipei, Taiwan, ROC, after obtaining informed consent (Institutional Review Board 1-101-105-97). The extracted fat was washed in three times in phosphate-buffered saline (GIBCO, Carlsbad, CA, USA)

and collected by centrifugation at $1200 \times g$ for 3 min each time. The tissue was then incubated in 0.075% type I collagenase (Sigma-Aldrich, St. Louis, MO, USA) for 1 h at 37°C, after which the collagenase was inactivated by addition of an equal volume of Dulbecco's modified Eagle's medium (Invitrogen Waltham, MA, USA) containing HyClone 10% fetal bovine serum (FBS; GE Healthcare Life Sciences, Chicago, IL, USA). The tissue was then centrifuged at $1200 \times g$ for 10 min, after which the pellet was collected as the stromal vascular fraction and cultured in keratinocyte-SFM (Invitrogen/GIBCO) containing 10% FBS, 1% penicillin-streptomycin (Invitrogen/GIBCO) and 1% glutamine (Invitrogen/GIBCO) at 37°C under 5% CO₂/95% air. After incubation for 1 day, the remaining red blood cells and unattached cells were washed away with Hanks buffered salt solution (HBSS; Thermo Scientific, Waltham, MA, USA), and the culture was continued by adding fresh medium. ADSCs were formed 3 days later and either subcultured or frozen for later use.

Flow Cytometry

Subcultured ADSCs (passage 3) were analyzed using flow cytometry. Aliquots of 1×10^7 ADSCs were suspended in PBS containing 0.5% bovine serum albumin (BSA; Bio-Rad Laboratories, Hercules, CA, USA), after which fluorescein isothiocyanate (FITC)-conjugated mouse anti-human CD73 (Thermo Fisher Scientific) and PE-conjugated mouse anti-human CD105 (Thermo Fisher Scientific) were added, and the suspension was incubated for 1 h on ice. The samples were then centrifuged and washed with PBS three times, suspended in 1 ml of PBS, and analyzed using a Becton Dickinson FACS Calibur (Franklin Lakes, NJ, USA). For each sample, 2.5×10^6 cells were retrieved and analyzed using CellQuest software.

Neurosphere Formation

To induce neurosphere formation, aliquots (5×10^5 cells) of passage 3 ADSCs were seeded into the Ultra-Low culture dishes (CORNING, Corning, NY, USA) and culture in NSC induction medium composed of keratinocyte-SFM containing 1% FBS, 1% penicillin-streptomycin, 1% glutamine, 20 ng/ml EGF (Invitrogen/GIBCO) and 20 ng/ml FGF (Peprotech, Rocky Hill, NJ, USA). The medium was changed every 2 days, and, after 7 days, the ADSCs developed into neurospheres.

Preparation of Acellular Tissue

The experimental procedures used in this study were reviewed and approved by the Institutional Animal Care and Use Committee (IACUC-16-114) of National Defense Medical Center, Taipei, Taiwan, ROC. Acellular tissue was prepared mainly as described previously^{16-18,23}. For the preparation of ADM, patches ($3 \times 5 \text{ cm}^2$) of full-thickness

skin were removed from 8- to 12-week-old nude mice (BALB/c-nu; BioLASCO Taiwan Co, Ltd, Taipei, Taiwan, ROC) and immersed in trypsin for 24 h at 37°C to remove the epidermis and other cells. The dermal matrix was then immersed in 0.5% Triton X-100 for 24 h at room temperature to form Trypsin-Triton ADM, which was washed five times in PBS and stored at 4°C in a refrigerator.

To obtain ASN, 8- to 12-week-old, male Sprague-Dawley rats (Blw: SD; BioLASCO) were sacrificed by CO₂ asphyxiation. ASN was then prepared from 25–30 mm of sciatic nerve collected from the freshly killed animals. After washing away residual blood with PBS, ASN was produced by soaking the nerve in 0.5% Triton X-100 at room temperature for 24 h with shaking (to remove cells). The resulting ASN was washed with PBS and stored at 4°C.

Immunofluorescent Staining

Tissue samples were immersed in OCT, frozen at –20 degrees, and cut into 10- μ m-thick sections. The sections were mounted on glass slides, which were washed three times with PBS, fixed for 30 min in 99% ethanol, treated for 30 min with PBS containing 0.05% Triton X-100, and blocked for 1 h in 2% normal goat serum (Cayman Chemical, Ann Arbor, MI, USA). The specimens were then incubated for 2 h with the primary antibody, washed with PBS, and incubated for 1.5 h with a secondary antibody at room temperature. The primary antibodies used in this study were mouse anti-Nestin monoclonal antibody (ab22035, 1:200; Abcam, Cambridge, UK), rabbit anti-Ki67 monoclonal antibody (ab16667, 1:200; Abcam), and mouse anti-SOX2 monoclonal antibody (MAB2018, 1:200; R&D Systems, Minneapolis, MN, USA). The secondary antibodies used were Alexa flour 488 goat anti-rabbit (Invitrogen/GIBCO) and Alexa Flour 594 goat anti-rat (Invitrogen/GIBCO). The specimens were then counterstained for 5 min with the nuclear dye 4',6-diamidino-2'-phenylindole (DAPI), wash with PBS, and covered with a coverslip, before being examined and imaged using a fluorescence microscope (Leica, Wetzlar, Hessen, Germany) or a Zeiss confocal laser scanning microscope (Carl Zeiss Inc, Thornwood, NY, USA).

NSCs Seeded onto ADM and ASN

Samples of ADM (1 cm²) and ASN (1 cm) were placed in the wells of a 24-well plate²³, after which 1×10^5 NSCs were added to each well and cultured on the ADM or ASN in NSC induction medium. After incubation for 72 h, unattached cells and medium were washed away with HBSS.

Sciatic Nerve Transection, Treatments, and Toluidine Blue Staining

To produce a rat model of sciatic nerve transection, 7- to 8-week-old (200–250 g) SD rats were anesthetized by intraperitoneal injection of 20 mg/kg Zoletil and 5 mg/kg

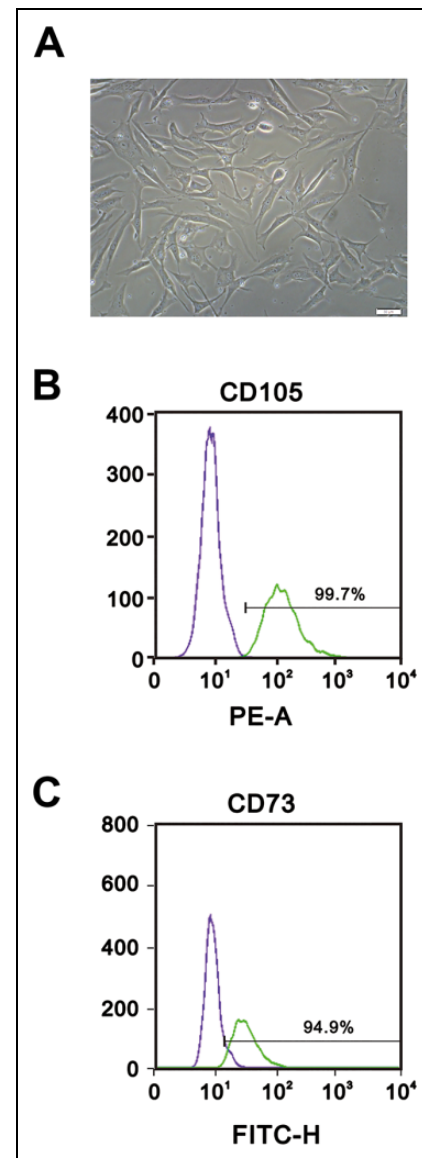


Fig. 1. Identification of human ADSCs. (A) Photomicrograph showing the morphology of ADSCs after 3 days in culture. Magnification, 20x; scale bar, 50 μ m. (B–C) The cell surface markers CD73 (B) and CD105 (C) were analyzed using flow cytometry.

Xylazine. After routine skin preparation and disinfection, incisions were made at the gluteal and posterior thigh to expose the left sciatic nerve, which was then transected at the middle portion of the nerve trunk to prepare a 10-mm nerve gap. The animals were randomly assigned to six groups: a sham operation group (sham) in which the sciatic nerve was explored but not damaged; a negative control (NG) group in which the sciatic nerve was left with the 10-mm gap but with no graft; ASN and ADM only groups in which the gaps were bridged using ASN or ADM; and ASN+N and ADM+N groups in which 5×10^5 cells dissociated from neurospheres were applied gaps bridged by ASN or ADM. After 8 weeks, the rats were sacrificed, and

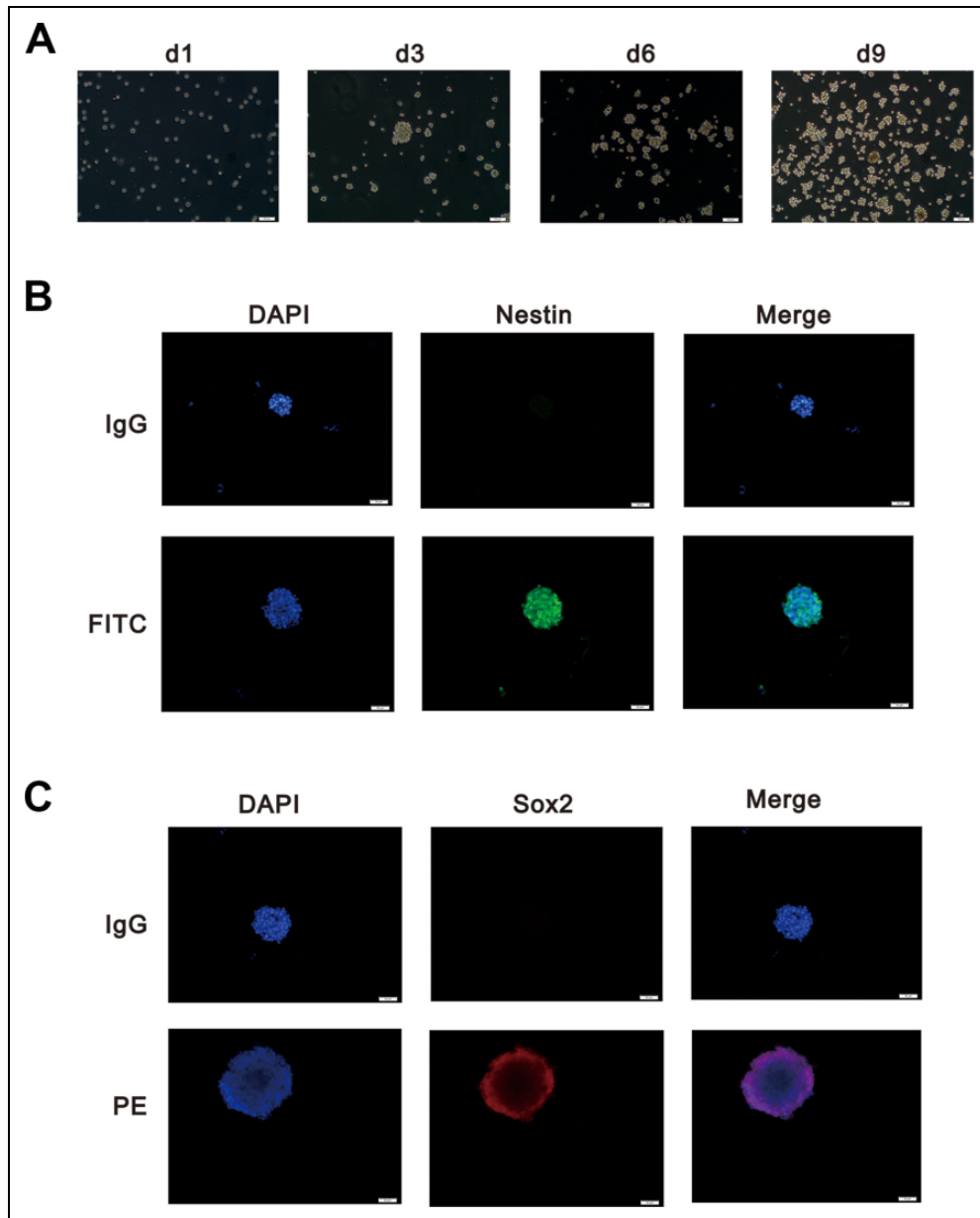


Fig. 2. Identification of NSCs. (A) Representative cell spheres dissociated into single cells, and culture was continued. After 3 days, the cells had re-aggregated, and the spheres proliferated with further culture. (B) Immunofluorescent staining of Nestin. Upper panels: IgG-treated negative controls, which show only nuclear staining with DAPI. Lower panels: Fluorescence images of FITC-labeled Nestin. (C) Immunofluorescent staining of Sox2. Upper panels: negative controls. Lower panels: Fluorescent images of PE-labeled Sox2. Scale bars, 50 μm in all panels.

the surgical sites were opened to harvest the nerve tissue and gastrocnemius.

The nerve grafts were transected using cryosection, each sheet having a thickness of 5 μm, followed by toluidine blue staining^{24–26}. The stock solution 1% toluidine blue (ScyTek Laboratory, Logan, UT, USA) was diluted to 0.1%, and each group was sectioned with a drop of 0.1% toluidine blue, allowed to stand for 1 min, and the slide was immersed in ionic water to wash away excess toluidine blue. The slides were dried at 60°C for at least 15 min, and covered with

a coverslip. Each group of slides was photographed under a microscope, and three photographs were randomly selected for each group. The number of axons per unit area was calculated using ImageJ software, version 1.44a (<http://imagej.nih.gov/ij/>), to calculate axonal density.

Sciatic Functional Index

Walking track analysis (footprint) and calculation of the Sciatic Functional Index (SFI) were as described by De

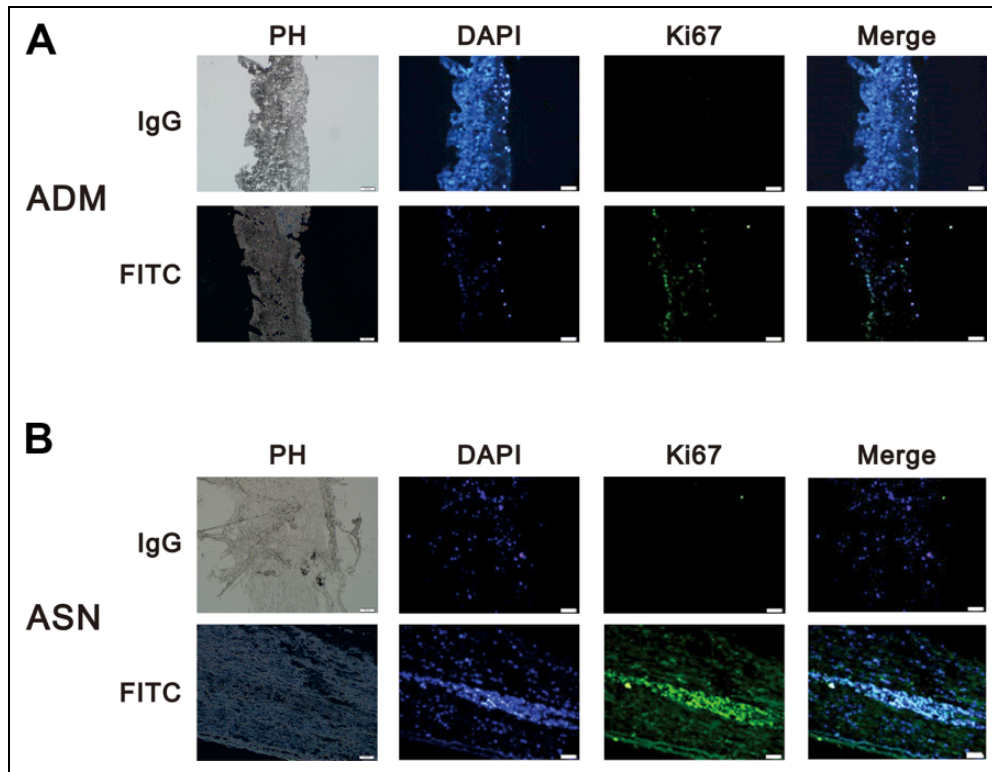


Fig. 3. ADM and ASN are suitable for NSC survival. (A and B) NSCs (1×10^5) were added to each well and cultured on ADM (A) or ASN (B) for 72 h. Upper panels: IgG-treated negative controls, which show only nuclear staining with DAPI. Lower panels: Fluorescence images showing FITC-labeled Ki67. Leftmost panels are phase contrast (PH) images of the tissue in white light. Scale bar, 50 μ m.

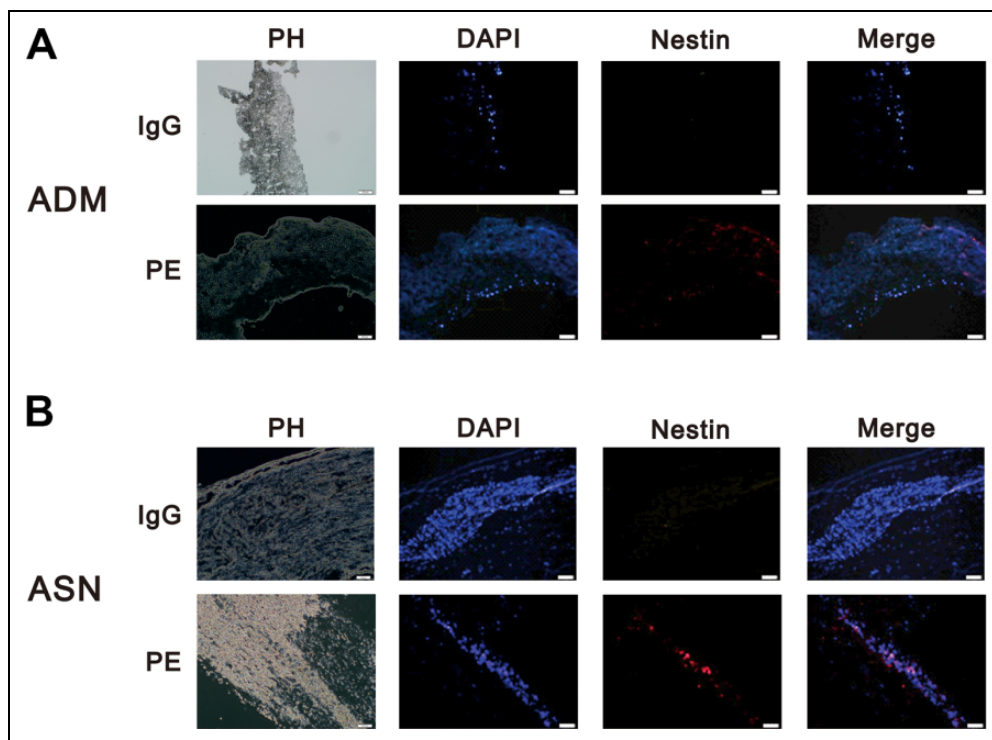


Fig. 4. NSCs seeded onto ADM exhibit surface markers of NSCs. (A and B) NSCs (1×10^5) were added to each well and cultured on ADM (A) or ASN (B) for 72 h. Upper panels: Negative controls, which show only nuclear staining with DAPI. Lower panels: Fluorescence images showing PE-labeled Nestin. Leftmost panels are phase contrast (PH) images of the tissue in white light. Scale bar 50 μ m.

Medinaceli et al²⁷. SD rats walked on an acrylic track that was 150 cm long, 13 cm wide, and 15 cm high. Ink and white paper were used to obtain the footprints, which were then photographed for analysis using ImageJ software. The SFI was then calculated from the footprint analysis using the following formula, as modified by Bain et al²⁸:

$$\text{SFI} = -38.8 \times \left(\frac{\text{EPL} - \text{NPL}}{\text{NPL}} \right) + 109.5 \times \left(\frac{\text{ETS} - \text{NTS}}{\text{NTS}} \right) + 13.3 \times \left(\frac{\text{EIT} - \text{NIT}}{\text{NIT}} \right) - 8.8$$

where E is experimental; N is normal; PL is the print length (distance between second toes and heel); TS is toe spread (distance between first and fifth toes); and IT is intermediate toe spread (the distance between the second and fourth toes).

Relative Gastrocnemius Muscle Weight

The gastrocnemius is the largest muscle dominantly innervated by the sciatic nerve in rats and usually begins to atrophy after nerve injury²⁹. The relative gastrocnemius muscle weight (RGMW) was used to assess nerve re-innervation. The RGMW was calculated from the ratio of the muscle weight on the injured side (left) to that on the healthy (right) side.

Histological Section Analysis

Samples of paraformaldehyde-fixed acellular tissue were dehydrated and embedded in paraffin. Transverse 5- μm -thick sections of ADM or ASN were then cut using a microtome and stained with hematoxylin and eosin (H&E) using standard histological procedures.

Statistical Analysis

Use the statistical software SigmaPlot 11 (Systat Software Inc., Chicago, IL, USA) to perform statistical analysis of the data. Data are expressed as means \pm SDs. A value of $p < 0.05$ was considered statistically significant.

Results

Characteristics of ADSCs and NSCs

Flow cytometric analysis of ADSCs like those shown in Fig. 1A revealed that about 99.7% of ADSCs expressed CD105, while about 94.6% expressed CD73 (Fig. 1B and C). The subcultured ADSCs (passage 3) were transferred to Ultra-low dishes for suspension culture in NSCs-inducing medium. After 7 days, the ADSCs had aggregated and taken on the morphology of neurospheres (Fig. 2), which were then dissociated into single cells using trypsin (Fig. 2A, d1). Within 3 days, the cells had re-aggregated into spheres (Fig. 2A, d3), which then proliferated over the course of the

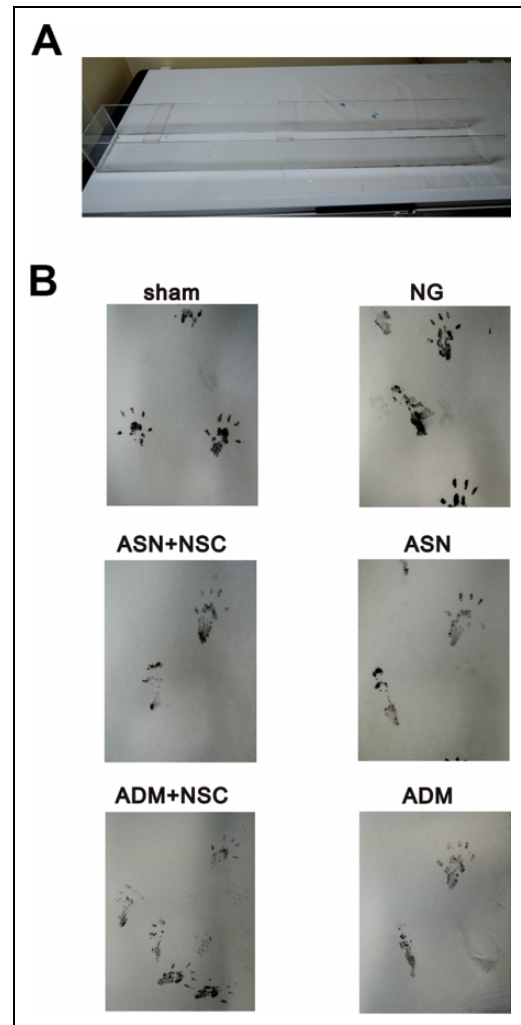


Fig. 5. Footprint analysis. (A) The walking path is a platform that is 150 cm long, 13 cm wide, and 15 cm high. (B) Representative footprints made by a rat from each of the indicated groups 8 weeks after transection of the left sciatic nerve leaving a 10 mm nerve gap.

next 6 days (Fig. 2A, d6 and d9). The fluorescence image in Fig. 2B and C show that the cells within the neurospheres expressed both Nestin and Sox2.

Confirmation that NSCs Can Survive on ADM and ASN

The two main methods for acellular tissue preparation are the freeze-thaw method and the chemical method. Previous research has shown that chemical de-cellularization helps to maintain the original structure of the tissue, which facilitates subsequent study^{16–18,30}. Here, we investigated whether NSCs could survive on ADM or ASN produced through chemical de-cellularization. NSCs were seeded onto ADM and injected into ASN; 3 days later, frozen sections were prepared and immunofluorescently stained for Ki67 to determine whether the cells could survive in ADM or ASN. We detected significant expression of Ki67 in both ADM and

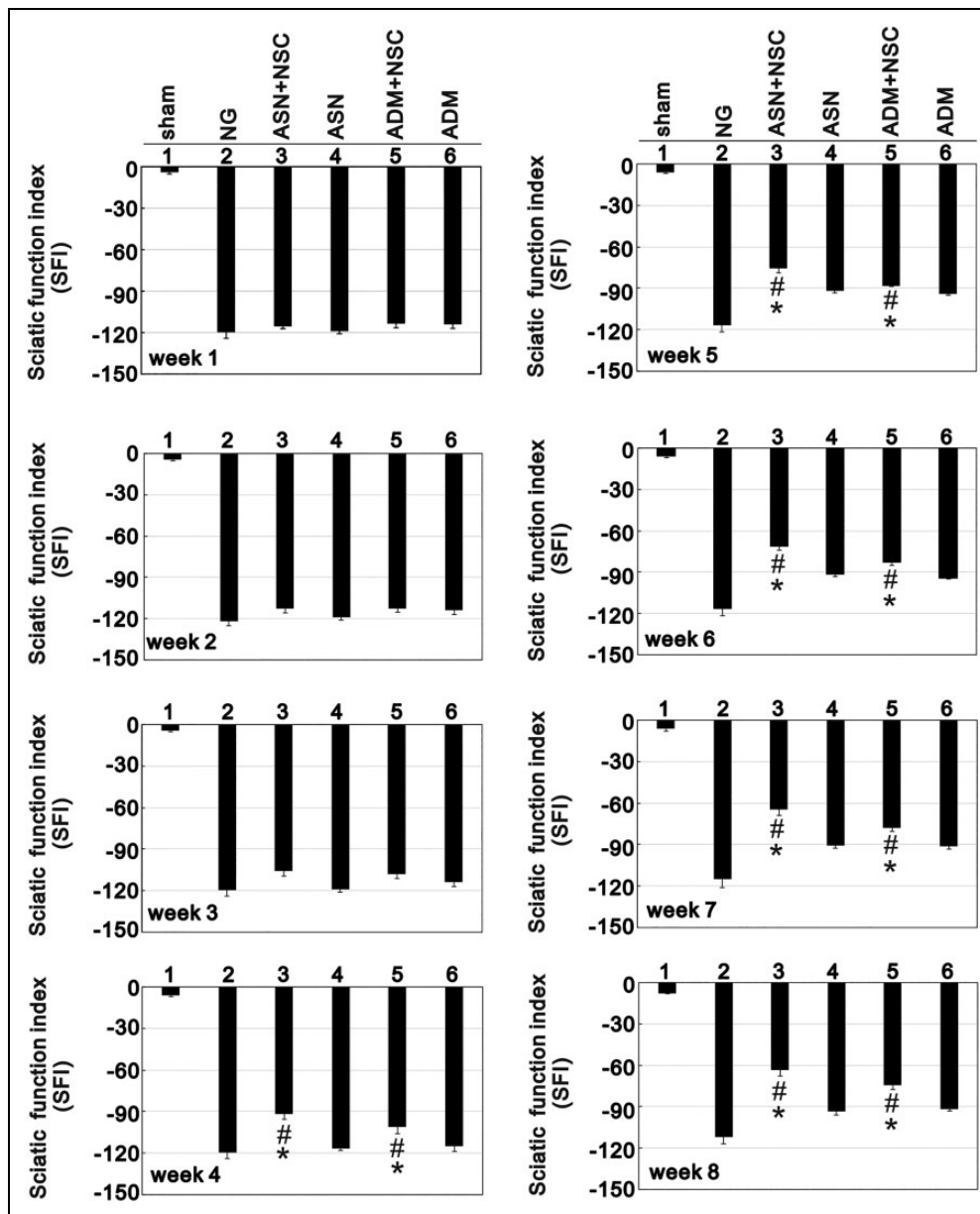


Fig. 6. Sciatic Functional Indexes (SFIs) recorded weekly for 8 weeks following left sciatic nerve transection. Bars depict the mean \pm SE. * $p < 0.001$ vs. the NG (NG), # $p < 0.01$ vs. the ASN only or ADM only group.

ASN, confirming that NSCs can survive in both ADM and ASN after chemical de-cellularization (Fig. 3A and B). The presence of Nestin confirmed that NSCs retain the characteristics of NSCs in both ADM and ASN (Fig. 4A and B).

Weekly Footprint Comparison

The track and representative footprints used to assess functional recovery 8 weeks after sciatic nerve transection leaving a 10 mm nerve gap are shown in Fig. 5. Using the SFI, we compared performance of injured hindlimb and the healthy contralateral hindlimb in the six groups of rats defined in the Methods: sham, NG, ASN only, ASN+NSC, ADM only,

and ADM+NSC (Fig. 6). SFIs greater than -100 indicate complete loss of nerve function. We found that from week 1 to week 3 the SFI in the sham group was significantly lower than in the other five groups, and there were no differences in SFI among the other groups. From week 4 to week 8, however, SFIs in the ASN+NSC and ADM+NSC groups were significantly lower than in the ASN only and ADM only groups, respectively. In addition, there was no significant difference between the ASN+NSC and ADM+NSC groups at week 4, but, from week 5 to week 8, although the SFIs in both groups showed a decreasing trend, the decline in the SFI was significantly greater in the ASN+NSC than ADM+NSC group.

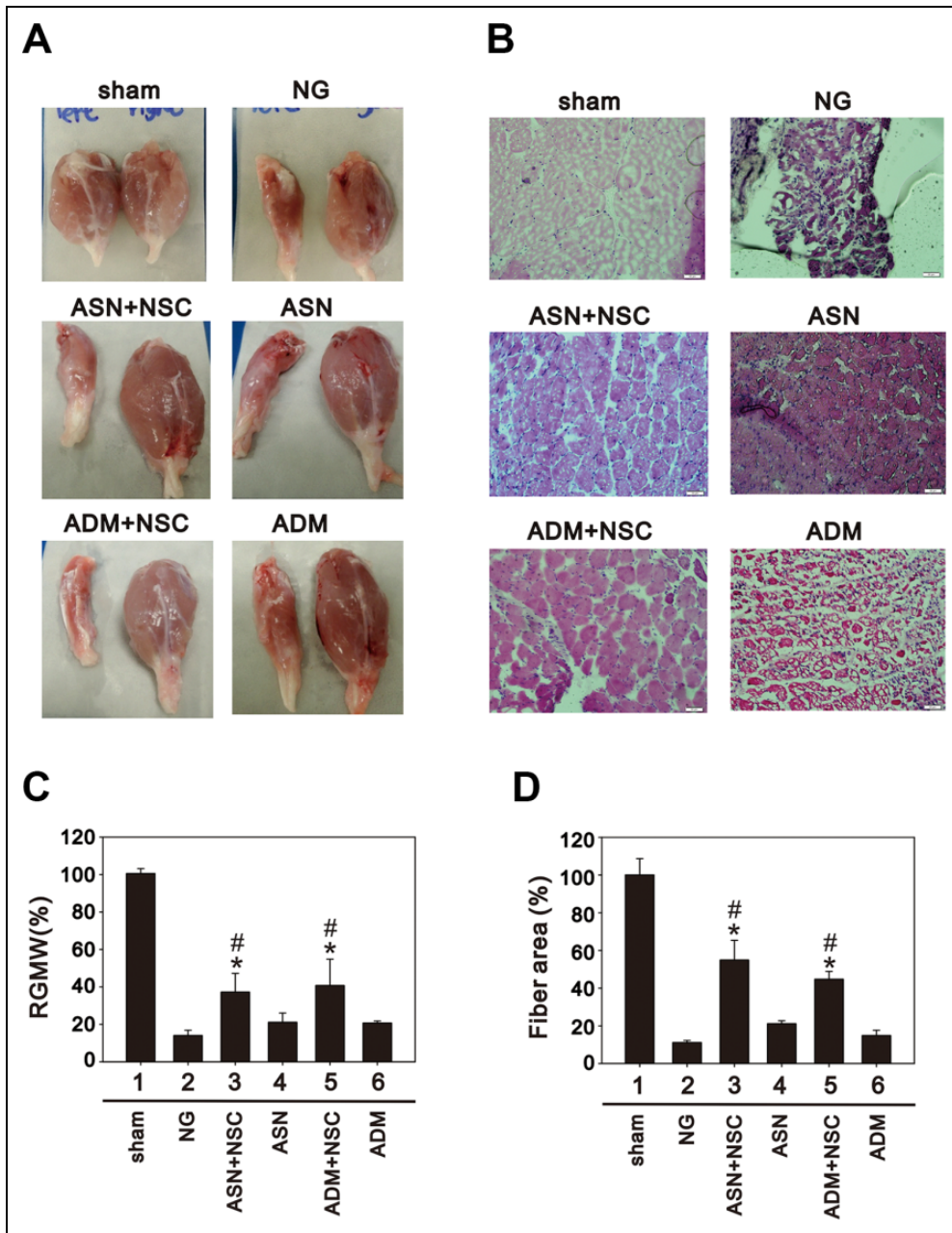


Fig. 7. Muscle atrophy assessed after 8 weeks of treatment. (A) Gastrocnemius muscles from surgically injured (left) and sham operated (right) hindlimbs in the indicated groups. (B) H&E-stained frozen sections of gastrocnemius muscle. (C and D) Relative gastrocnemius muscle weight (RGMW) (C) and relative muscle fiber cross-sectional areas (D) used to compare the injured and sham operated hindlimbs in the indicated groups. Values are expressed as percentages of those in the sham group. Bars depict the mean \pm SE. * $p < 0.001$ vs. NG, # $p < 0.01$ vs. ASN only or ADM only group.

Comparison of Muscle Atrophy and Muscle Fiber Area

Because sciatic nerve transection leads to atrophy of the gastrocnemius muscle, the RGMW and cross-sectional muscle fiber areas were compared between the injured (left) and sham operated (right) sides in the six experimental groups. After 8 weeks of treatment, the gastrocnemius muscle in the NG group was obviously atrophied (Fig. 7A and B), while the RGMWs in the ADM+N and ASN+N groups were both

significantly greater than in the other groups, indicating less muscle atrophy (Fig. 7C). Likewise, cross-sectional muscle fiber areas were significantly greater in the ADM+N and ASN+N groups than in the NG, ADM only, or ASN only group (Fig. 7D). For both RGMW and cross-sectional muscle fiber area, there was no significant difference between the ADM+N and ASN+N groups. It thus appears that ADM+N and ASN+N both exerted significant protective

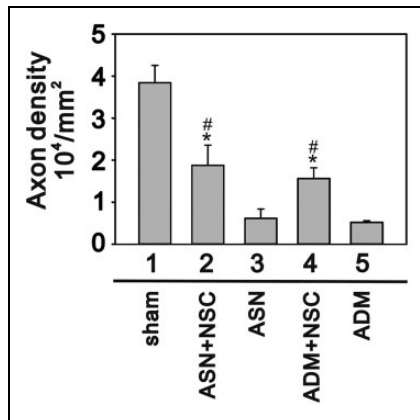


Fig. 8. Axon density analysis. Left sciatic nerves from rats in the indicated groups were excised, sectioned and stained with toluidine blue to calculate the number of axons per unit area. Bars depict the mean \pm SE. * $p < 0.001$ vs. sham, # $p < 0.01$ vs. the ASN only or ADM only group.

effects against gastrocnemius muscle atrophy and that the two treatments were equally effective.

Combining ADM or ASN with NSCs Enhances Axonal Regeneration

After 8 weeks of treatment, the rats in each group were sacrificed, and the sciatic nerve was sectioned and stained. The axon density was assessed by toluidine blue stain (Fig. 8). We found that the axon densities in the ADM+N and ASN+N groups were significantly higher than in the ADM only and ASN only groups, but they did not differ from one another.

Discussion

According to Seddon's classification of peripheral nerve injury, the nerve gap belongs to the highest level of nerve damage^{31,32}. From a clinical viewpoint, the conditions associated with a nerve gap that affect nerve repair status are the location of the nerve defects, the length of the affected region, and the diameter of the affected nerve. Current medical technology can be used to transplant autologous sensory nerves, but in addition to the limited numbers of compatible transplant donors, the procedure causes paralysis at the donor site. In the present study, we focused on the use of ADM in combination with ADSC-derived NSCs in an effort to assess the advantage of its plasticity and ductility for sciatic nerve repair. Our results indicate that treatment with ADM+NSC improved gastrocnemius weight, cross-sectional fiber areas, and SFI as effectively as the currently used ASN+NSC. At present, neuro-engineered artificial and biomimetic materials or acellular nerves cannot completely reverse long nerve defects. It is hoped that the combination of ADM and stem cells may provide a new and effective choice for treatment.

According to Waller's degeneration model, there are three main stages of peripheral nerve damage. First, Schwann cells are released from the myelin sheath and proliferate in the basal lamina. Then, damaged axons and free Schwann cells release various cytokines. Finally, the damaged axons form a growth cone and begin to regenerate along the Büngner zone formed by the Schwann cells^{11,32}. Peripheral nerve damage may involve different cells or growth factors at different times. In addition to myelin growth and nerve regeneration, the microenvironment of the nerve damage may affect the role of NSCs³³. The inflammatory process associated with nerve damage likely affects NSC differentiation and lasts for about a week. This may explain why there was little change in SFI in the ASN+NSC and ADM+NSC groups during the first 3 weeks of treatment (Fig. 6). In addition, the substantial improvements that began in week 4 slowed after week 7. This suggests the timing of ADM-NSC therapy is an important issue for nerve repair and may be a key factor affecting outcome. Determination of the optimal therapeutic time course will need to be an objective of future studies. It will also be necessary to investigate the distribution of injected NSCs. Our findings indicate NSCs survive in the lumen of ADM, but we know little about how the cells were distributed after injection, or even how many stayed at the site of nerve damage. One approach to addressing this issue may be to mix NSCs with a gelatinous substance, which could be injected into the lumen of the ADM at appropriate sites for treatment of nerve defects and which would retain the cells in that region.

Nerve damage repair also involves the generation of a blood–neural barrier, which is a network of blood vessels formed by endothelial cells that surrounds the nerve bundle to provide protection and nutrients³⁴. ADSCs can be induced to form vascular endothelial cells³⁵. Perhaps it would be effective to mix ADSC-derived NSCs and peripheral nerve microvascular endothelial cells when treating nerve gaps, but that remains to be tested. In addition, platelet rich plasma (PRP) is known to be clinically useful for wound healing and joint repair. In recent years, PRP has also shown potential to contribute to nerve repair. This suggests further improvement of nerve damage repair may be achieved by adding various platelet-associated growth factors and mediators, such as platelet-derived growth factor-AA, which our laboratory recently reported acts on ADSCs and endothelial progenitor cells to enhance wound healing in a rat model³⁶.

Conclusions

In summary, our findings suggest that ADSC-derived NSCs can be combined with ADM to enhance the repair of peripheral nerve defects. Although our results indicate that ADM combined with NSCs can improve peripheral nerve gap repair after nerve transection, the ductility and plasticity of ADM may enable it to also effectively serve as a nerve bridge facilitating the repair of other types of neurological gaps.

Ethical Approval

The source of ADSC was 10 healthy male and female donors who had undergone surgery at Tri-Service General Hospital (TSGH) in Taipei, Taiwan, ROC. The hospital obtained informed consent from each of the donors (Institutional Review Board 1-101-105-97)

Statement of Human and Animal Rights

ADSCs were provided by TSGH. Male Sprague-Dawley rats and BALB/c-nu nude mice were used in this study. All experimental procedures were reviewed and approved by the Institutional Animal Care and Use Committee (IACUC-16-114).

Statement of Informed Consent

The source of ADSCs was 10 healthy male and female donors who had undergone surgery at TSGH. The hospital obtained informed consent from each of the donors (Institutional Review Board 1-101-105-97)


Declaration of Conflicting Interests

The author(s) declared no potential conflicts of interest with respect to the research, authorship, and/or publication of this article.

Funding

The author(s) disclosed receipt of the following financial support for the research and/or authorship of this article: The work was supported in part by grants from the Ministry of Science and Technology (MOST 106-2314-B-016-025 and MOST 107-2314-B-016-034) and by a grant from Tri-Service General Hospital (TSGH-C107-118), Taiwan, ROC.

ORCID iD

Shih-Ming Huang  <https://orcid.org/0000-0001-9305-921X>

References

- Daly W, Yao L, Zeugolis D, Windebank A, Pandit A. A biomaterials approach to peripheral nerve regeneration: bridging the peripheral nerve gap and enhancing functional recovery. *J R Soc Interface*. 2011;96(7):202–221.
- Sachanandani NF, Pothula A, Tung TH. Nerve gaps. *Plast Reconstr Surg*. 2014;133(2):313–319.
- Dahlin L. Techniques of peripheral nerve repair. *Scand J Surg*. 2008;97(4):310–316.
- Isaacs J, Browne T. Overcoming short gaps in peripheral nerve repair: conduits and human acellular nerve allograft. *Hand*. 2014;9(2):131–137.
- Grinsell D, Keating C. Peripheral nerve reconstruction after injury: a review of clinical and experimental therapies. *Biomed Res Int*. 2014;2014:698256.
- Habre SB, Bond G, Jing XL, Kostopoulos E, Wallace RD, Konofaos P. The surgical management of nerve gaps: present and future. *Ann Plast Surg*. 2018;80(3):252–261.
- Humphries MJ, Akiyama SK, Komoriya A, Olden K, Yamada KM. Neurite extension of chicken peripheral nervous system neurons on fibronectin: relative importance of specific adhesion sites in the central cell-binding domain and the alternatively spliced type III connecting segment. *J Cell Biol*. 1988;106(4):1289–1297.
- Szynkaruk M, Kemp SW, Wood MD, Gordon T, Borschel GH. Experimental and clinical evidence for use of decellularized nerve allografts in peripheral nerve gap reconstruction. *Tissue Eng Part B Rev*. 2012;19(1):83–96.
- Moore AM, MacEwan M, Santosa KB, Chenard KE, Ray WZ, Hunter DA, Mackinnon SE, Johnson PJ. Acellular nerve allografts in peripheral nerve regeneration: a comparative study. *Muscle Nerve*. 2011;44(2):221–234.
- Jiang L, Jones S, Jia X. Stem cell transplantation for peripheral nerve regeneration: current options and opportunities. *Int J Mol Sci*. 2017;18(1):94.
- Gaudet AD, Popovich PG, Ramer MS. Wallerian degeneration: gaining perspective on inflammatory events after peripheral nerve injury. *J Neuroinflammation*. 2011;8(1):110.
- Lee D-C, Chen J-H, Hsu T-Y, Chang L-H, Chang H, Chi Y-H, Chiu M. Neural stem cells promote nerve regeneration through IL12-induced Schwann cell differentiation. *Mol Cell Neurosci*. 2017;79:1–11.
- Ernst A, Alkass K, Bernard S, Salehpour M, Perl S, Tisdale J, Possnert G, Druid H, Frisén J. Neurogenesis in the striatum of the adult human brain. *Cell*. 2014;156(5):1072–1083.
- Strem BM, Hicok KC, Zhu M, Wulur I, Alfonso Z, Schreiber RE, Fraser JK, Hedrick MH. Multipotential differentiation of adipose tissue-derived stem cells. *Keio J Med*. 2005;54(3):132–141.
- Hsueh Y-Y, Chang Y-J, Huang T-C, Fan S-C, Wang D-H, Chen J-J, Wu C-C, Lin S-C. Functional recoveries of sciatic nerve regeneration by combining chitosan-coated conduit and neurosphere cells induced from adipose-derived stem cells. *Biomaterials*. 2014;35(7):2234–2244.
- Castagnoli C, Fumagalli M, Alotto D, Cambieri I, Casarin S, Ostorero A, Casimiri R, Germano P, Pezzuto C, Stella M. Preparation and characterization of a novel skin substitute. *J Biomed Biotechnol*. 2010;2010:840363.
- Chen X, Feng X, Xie J, Ruan S, Lin Y, Lin Z, Shen R, Zhang F. Application of acellular dermal xenografts in full-thickness skin burns. *Exp Ther Med*. 2013;6(1):194–198.
- Walter RJ, Matsuda T, Reyes HM, Walter JM, Hanumadass M. Characterization of acellular dermal matrices (ADMs) prepared by two different methods. *Burns*. 1998;24(2):104–113.
- Nilsen TJ, Dasgupta A, Huang Y-C, Wilson H, Chnari E. Do processing methods make a difference in acellular dermal matrix properties? *Aesthet Surg J*. 2016;36(suppl_2):S7–S22.
- Carruthers CA, Dearth CL, Reing JE, Kramer CR, Gagne DH, Crapo PM, Garcia Jr O, Badhwar A, Scott JR, Badylak SF. Histologic characterization of acellular dermal matrices in a porcine model of tissue expander breast reconstruction. *Tissue Eng Part A*. 2014;21(1–2):35–44.
- Pabst A, Happe A, Callaway A, Ziebart T, Stratul S, Ackermann M, Konerding M, Willershausen B, Kasaj A. In vitro and in vivo characterization of porcine acellular dermal matrix for gingival augmentation procedures. *J Periodontol Res*. 2014;49(3):371–381.
- Lindman JP, Talbert M, Zhang W, Powell B, Accortt NA, Rosenthal EL. Promotion of acellular dermal matrix resolution in vitro by matrix metalloproteinase-2. *Arch Facial Plast Surg*. 2006;8(3):208–212.

23. Syu WZ, Chen SG, Chan JY, Wang CH, Dai NT, Huang SM. The potential of acellular dermal matrix combined with neural stem cells induced from human adipose-derived stem cells in nerve tissue engineering. *Ann Plast Surg.* 2019;82(1 S Suppl 1):S108–S118.
24. Carriel V, Garzón I, Alaminos M, Cornelissen M. Histological assessment in peripheral nerve tissue engineering. *Neural Regen Res.* 2014;9(18):1657–1660.
25. Lee SH, Jin W-P, Seo NR, Pang K-M, Kim B, Kim S-M, Lee J-H. Recombinant human fibroblast growth factor-2 promotes nerve regeneration and functional recovery after mental nerve crush injury. *Neural Regen Res.* 2017;12(4):629–636.
26. Ghnenis AB, Czaikowski RE, Zhang ZJ, Bushman JS. Toluidine blue staining of resin-embedded sections for evaluation of peripheral nerve morphology. *J Vis Exp.* 2018;(137):e58031.
27. de Medinaceli L, Freed WJ, Wyatt RJ. An index of the functional condition of rat sciatic nerve based on measurements made from walking tracks. *Exp Neurol.* 1982;77(3):634–643.
28. Bain JR, Mackinnon SE, Hunter DA. Functional evaluation of complete sciatic, peroneal, and posterior tibial nerve lesions in the rat. *Plast Reconstr Surg.* 1989;83(1):129–138.
29. Staron RS, Kraemer WJ, Hikida RS, Fry AC, Murray JD, Campos GE. Fiber type composition of four hindlimb muscles of adult Fisher 344 rats. *Histochem Cell Biol.* 1999;111(2):117–123.
30. Balasubramani M, Kumar TR, Babu M. Skin substitutes: a review. *Burns.* 2001;27(5):534–544.
31. Seddon H. A classification of nerve injuries. *Br Med J.* 1942;2(4260):237–239.
32. Deumens R, Bozkurt A, Meek MF, Marcus MA, Joosten EA, Weis J, Brook GA. Repairing injured peripheral nerves: bridging the gap. *Prog Neurobiol.* 2010;92(3):245–276.
33. Zhao Y, Xiao Z, Chen B, Dai J. The neuronal differentiation microenvironment is essential for spinal cord injury repair. *Organogenesis.* 2017;13(3):63–70.
34. Choi Y-K, Kim K-W. Blood-neural barrier: its diversity and coordinated cell-to-cell communication. *BMB Rep.* 2008;41(5):345–352.
35. Deng M, Gu Y, Liu Z, Qi Y, Ma GE, Kang N. Endothelial differentiation of human adipose-derived stem cells on polyglycolic acid/polylactic acid mesh. *Stem Cells Int.* 2015;2015:350718.
36. Wu LW, Chen WL, Huang SM, Chan JYH. Platelet-derived growth factor-A A is a substantial factor in the ability of adipose-derived stem cells and endothelial progenitor cells to enhance wound healing. *FASEB J.* 2019;33(2):2388–2395.